Organic Geochemistry 113 (2017) 105–114

Contents lists available at ScienceDirect

Organic Geochemistry

journal homepage: www.elsevier.com/locate/orggeochem

Holocene climate change in northeastern China reconstructed from lipid biomarkers in a peat sequence from the Sanjiang Plain

Yan Zhang [a,d], Philip A. Meyers [c], Chuanyu Gao [b], Xingtu Liu [b], Jian Wang [b], Guoping Wang [b,*]

[a] Key Laboratory of Humid Subtropical Eco-geographical Process, Ministry of Education, FujianNormal University, Fuzhou 350007, China
[b] Key Laboratory of Wetland Ecology and Environment, Northeast Institute of Geography and Agroecology, Chinese Academy of Sciences, Changchun 130102, China
[c] Department of Earth and Environmental Sciences, The University of Michigan, Ann Arbor, Michigan 48109-1005, USA
[d] Research Centre of Wetlands in Subtropical Region, Institute of Geographical Sciences, Fujian Normal University, Fuzhou 350007, China

ARTICLE INFO

Article history:
Received 4 January 2017
Received in revised form 22 June 2017
Accepted 31 July 2017
Available online 9 August 2017

Keywords:
Peat
n-Alkanes
n-Fatty acids
Holocene climate
Sanjiang Plain

ABSTRACT

Lipid biomarkers extracted from a sediment-peat sequence from the Sanjiang Plain were analyzed to assess the change in regional vegetation and climate during the last 8 ky. The combination of *n*-alkane and *n*-alkanoic acid distributions and published pollen and plant macrofossil records for the lake sediments underlying the peat reveal that the region experienced a warmer and wetter period before ca. 6 ka that corresponds to the monsoon maximum and Holocene climate optimum in northeast China. The climate then entered a cold and wet period from 6 to 4 ka. A shift to warmer and drier conditions starting 4 ka is recorded as a transformation from a shallow lake to a peat deposit. From 1.5 to 0.4 ka, the region entered a cold and wet period that was followed by warm and dry conditions for the most recent 0.4 ky. Our lipid-based paleoclimate reconstruction was compared with Holocene reconstructions based on lipid records from the nearby Hani peat sequence, peat cellulose $\delta^{13}C$ results from the Jinchuan peat sequence, and pollen records from other lakes in northeast China. Most of the regional paleoclimate changes reconstructed from the lipid proxies in the Sanjiang Plain peat sequence have a strong link with sea surface temperature changes in the Sea of Japan that were influenced by summer solar insolation at 65°N and the East Asia summer monsoon. In contrast, the change to the warmer and drier conditions of the last four centuries seems to be mainly a consequence of human activity.

1. Introduction

Peat comprises the preserved remains of plants that grow in bogs and fens. Both the kinds of plants that contribute to the peat and the post-depositional microbial alteration of the plant residues are sensitive to changes in climate (Zheng et al., 2007; Zhou et al., 2010). Hence, undisturbed peat sequences can provide high resolution archives of past climate change (Blackford, 2000).

The lipid composition of peat sequences is recognized as containing important proxies for providing information on climate-caused changes in the communities of plants that contribute to peat accumulation and on the alteration that peat deposits may experience after formation. Compared with some other paleoclimate proxies, biomarkers are more valuable for reflecting past environmental change because of their special features of relative source specificity and recalcitrance (Zhang Y. et al., 2014, 2016). Different types of peat-forming plants produce distinctive carbon chain length distributions of lipids (Cranwell, 1973). In general, *Sphagnum* spp. and submerged and floating aquatic vascular plants are characterized by mid-chain (C_{23} and C_{25}) *n*-alkanes, and terrigenous higher plants are dominated mainly by long chain (C_{27}, C_{29} and C_{31}) *n*-alkanes (e.g. Cranwell, 1973, 1984; Ficken et al., 1998; Nott et al., 2000; Bass et al., 2000; Nichols et al., 2006; Bingham et al., 2010). For *n*-fatty acids (*n*-FAs), short chain (C_{14}, C_{16} and C_{18}) components are abundant in aquatic algae or bacteria, whereas terrigenous higher plants synthesize abundant even long chain (C_{24}, C_{26} and C_{28}) homologues (Cranwell, 1973). Therefore, lipid ratios including the carbon preference index (CPI), average chain length (ACL), proportion of aqueous biomarkers (P_{aq}), and some other lipid biomarker proxies have been applied successfully to infer the types of peat-forming plant inputs and thereby to reflect regional climate change (e.g. Nott et al., 2000; Xie et al., 2004; Zhou et al., 2005, 2010; Zhang et al., 2006; Zheng et al., 2007; Andersson et al., 2011; Y. Zhang et al., 2014, 2016).

The peat bogs that are widely distributed in northeast China have provided special archives for regional paleoenvironmental reconstruction. Studies of the paleoclimate record of the region

* Corresponding author. Fax: +86 431 8554229.
E-mail address: wangguoping@neigae.ac.cn (G. Wang).

http://dx.doi.org/10.1016/j.orggeochem.2017.07.018
0146-6380/

have focused mainly on the Hani peatland that has yielded particularly useful information from its peat cellulose $\delta^{13}C$ and $\delta^{18}O$ values (Hong et al., 2005, 2009), lipid biomarker distributions (Zhou et al., 2010), *n*-alkane δD values (Seki et al., 2009) and *n*-alkane $\delta^{13}C$ values (Yamamoto et al., 2010). Additional paleoclimate information has been obtained from peat cellulose $\delta^{18}O$ and $\delta^{13}C$ values in the nearby Jinchuan peat sequence (Hong et al., 2001). In addition, *n*-alkanes and pollen in the Great Hinggan Mountain ombrotrophic peat bog at the northern edge of the East Asian monsoon margin in northeastern China have been used to reconstruct the succession of local vegetation communities and thereby reconstruct change in regional climate over the past 1 ky (Lin et al., 2004; Y. Zhang et al., 2014). Climate change in northeast China is mainly influenced by the East Asian Monsoon. Most of the regional precipitation falls during the summers when annual temperature peaks and plays an important role in peat accumulation. Therefore, undisturbed peat sequences in northeast China can serve as good archives for reconstructing the relationship between regional climate change and East Asia summer monsoon variation.

The Sanjiang Plain (43°49′–48°27′N; 129°11′–135°05′E) lies in northeastern China. It is a huge alluvial plain deposited by three major rivers (Heilong, Wusuli, and Songhua) and is the largest wetland in China. Well preserved peatlands in the region have accumulated in dish-like depressions at different rates during the Holocene (Liu, 1995; Z. Zhang et al., 2014, 2016). Therefore, the peat in the plain can serve as a valuable geological archive for providing evidence for regional climate change. Only Wang et al. (2015) and Z. Zhang et al. (2014, 2016) have reconstructed the history of peat deposition and water level change from these peat records. Their reconstructions are based on plant microfossil and pollen data and total organic carbon (TOC) accumulation rate. We present here a record of TOC and lipid biomarkers in a peat sequence from the plain to provide a more detailed reconstruction of the change in regional climate during the middle and late Holocene. By comparison with other climate records, we offer a comprehensive interpretation that relates the regional climate change in northeast China with change in sea surface temperature (SST) of the Sea of Japan and evolution of regional humidity associated with the East Asian summer monsoon.

2. Material and methods

2.1. Study site

The Shen Jiadian (SJD) peatland (46°34.864′N, 130°39.873′E; ca. 165 m above sea level, asl) is on the southern Sanjiang Plain in Heilongjiang Province, northeast China (Fig. 1). Mean annual air temperature in the region is 2.5 °C, with an average maximum of 22 °C in July and a minimum of −18 °C in January; the total annual precipitation is ca. 500–600 mm and is concentrated mainly in May to September. The modern vegetation cover is dominated by sedge communities (*Calamagrostis angustifolia, Carex lasiocarpa*, and *Carex pseudocuraica*), accompanied by shrubs (*Salix myrtilloides, Salix brachypoda*) and *Sphagnum* spp. (Wang et al., 2015).

2.2. Sample collection and stratigraphy

The peatland exists as a dish-like structure in the study region. Z. Zhang et al. (2014) have described the Quaternary lithological strata in detail with a schematic diagram. A sequence (195 cm) was collected from an artificial outcrop in a dish-like basin by drilling with a Wardennar peat sampler in September, 2010. The stratigraphy of the sequence contained two distinctive layers based on color and fossil roots; the top 165 cm was composed of brown peat, and the bottom from 165 cm to 195 cm was black mud peat (Fig. 2). The core was divided into 195 samples on-site by slicing into 1 cm intervals that were stored in polyethylene bags and transported to the laboratory for analysis.

2.3. Chronology of peat-mud sequence

For the chronology, 8 bulk peat samples (roots removed) were analyzed at the radiocarbon dating laboratories of Xi'an Institute of Earth Environment (Chinese Academy of Sciences) using AMS ^{14}C dating (Z. Zhang et al., 2014; Wang et al., 2015), and the radiocarbon ages were calibrated to calendar ages using CALIB Rev.7.0.1 software (Table 1). The chronology of the sequence was calculated using the cubic-spline method based on the 8 calibrated calendar age values (Fig. 2). Peat accumulation rate (PAR) values were

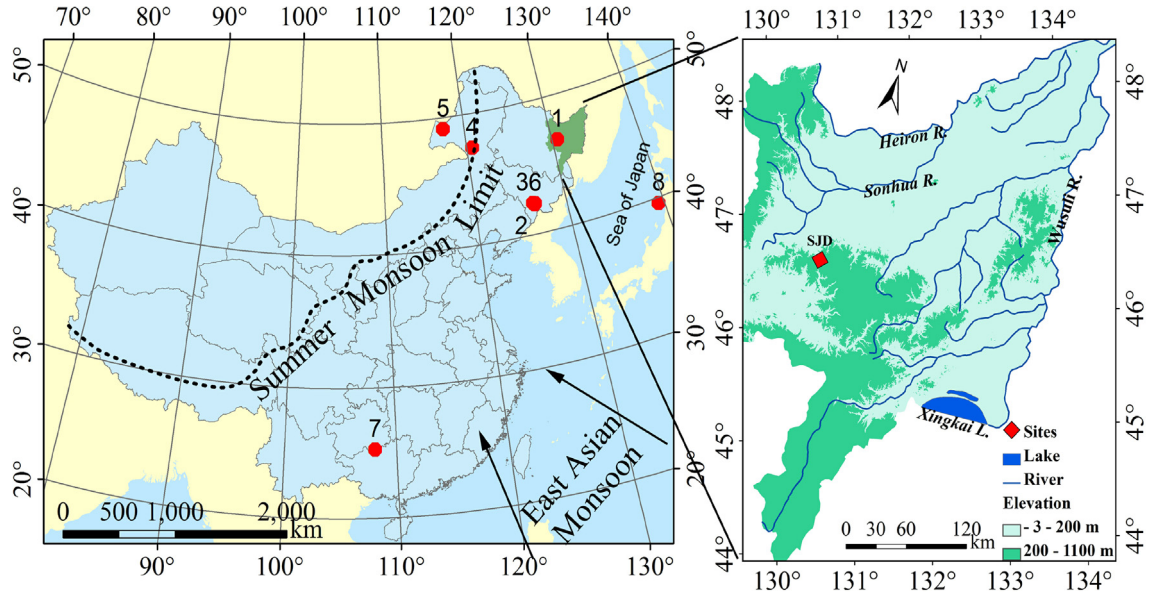

Fig. 1. Location of SJD peatland in the Sanjiang Plain, northeast China and other sites mentioned in the text. 1, SJD peatland (current study); 2, Hani peatland (Zhou et al., 2010); 3, Jinchuan peatland (Hong et al., 2001) 4, Great Hinggan ombrotrophic peat bog (Y. Zhang et al., 2014); 5, Hulun Lake (Wen et al., 2010); 6, Sihailongwan Lake (Stebich et al., 2015); 7, Stalagmite record of Dongge Cave from Guizhou province, China (Wang et al., 2005); 8, sea surface temperature (SST) data for Japan Sea based on a sediment core from the sea (Ishiwatari et al., 2001).

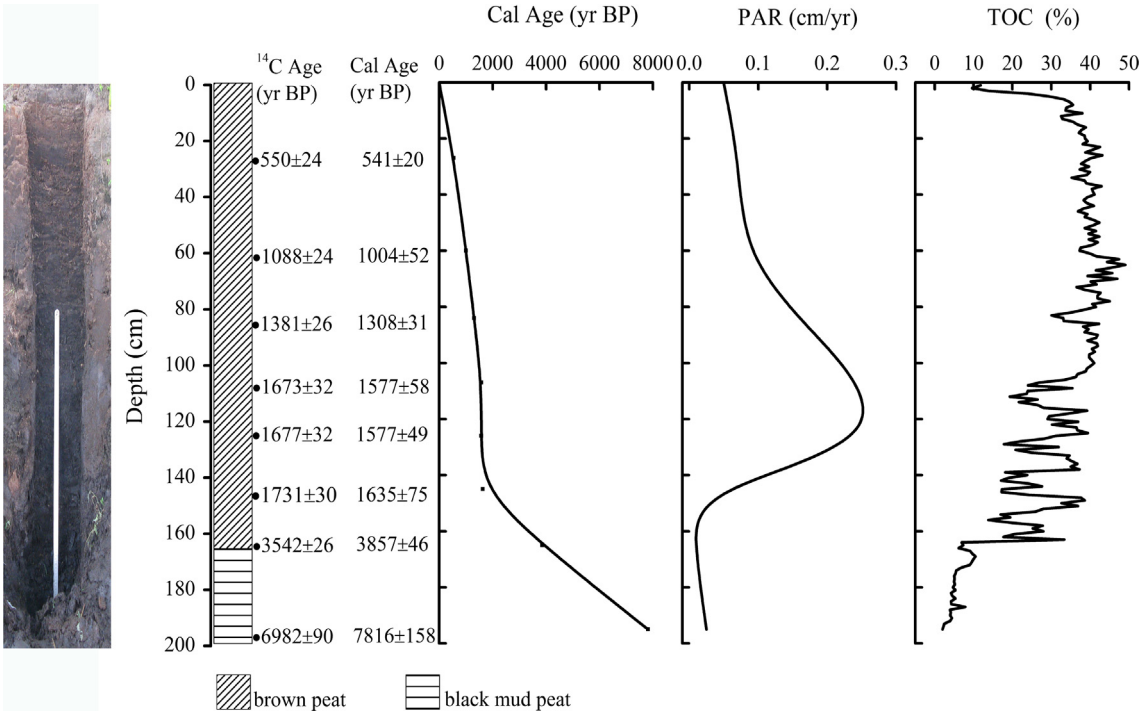

Fig. 2. Lithostratigraphy, age-depth relationship, PAR and TOC concentration for the 195 cm core from the SJD peat sequence. TOC concentration from Z. Zhang et al. (2014).

Table 1
Radiocarbon and calibrated age data for SJD peat sequence in Sanjiang Plain.

Lab number[a]	Depth (cm)	Material dated	AMS ^{14}C age (yr BP)	Calibrated ^{14}C age (cal yr BP)	Error (± 2 σ) (cal yr BP)
XA-7553	27	Bulk peat	550 ± 24	521–560	20
XA-7592	60	Bulk peat	1088 ± 24	937–1013	52
XA-7542	84	Bulk peat	1381 ± 26	1277–1336	31
XA-7543	107	Bulk peat	1673 ± 32	1524–1630	58
XA-7554	126	Bulk peat	1677 ± 23	1533–1620	49
XA-7555	145	Bulk peat	1731 ± 30	1564–1708	75
XA-7570	165	Bulk peat	3542 ± 26	3811–3900	46
XA-7571	195	Bulk peat	6982 ± 90	7658–7972	158

[a] XA, Xi'an Institute of Earth Environment, Chinese Academy of Sciences.

estimated from the calculated calendar ages and the corresponding depth intervals (Fig. 2).

2.4. Lipid analysis

Samples were taken at 5 cm intervals, freeze-dried and ground to < 80 mesh. Total lipids were extracted 5x from dried aliquots (1 g) with 20 ml $CHCl_3$ in an ultrasonic extractor for 15 min. The extracts were combined and concentrated in a rotary evaporator. The dried extracts were dissolved in *n*-hexane; the saturated hydrocarbon, aromatic hydrocarbon and non-hydrocarbon fractions were isolated using silica gel column chromatography (60 mesh) by way of sequential elution with 20 ml *n*-hexane, benzene, and MeOH, respectively. The eluate was concentrated with a N_2 stream, and the saturated hydrocarbon fraction was transferred to a vial and directly analyzed using gas chromatography-mass spectrometry (GC–MS), whereas the non-hydrocarbon fraction was derivatized with N,O-bis(trimethylsilyl)trifluoroacetamide (BSTFA) by heating at 70 °C for 1.5 h before GC–MS analysis.

Quantification of lipids was carried out using GC–MS with a Shimadzu QP5050A system equipped with a DB-5MS fused quartz column (30 m × 0.25 mm × 0.25 μm). The temperature of the ion source was 250 °C, and the ionization energy was 70 eV, with He as carrier gas. GC operating conditions were: 80 °C to 175 °C at 3 °C/min, then heating to 300 °C (held 20 min) at 4 °C/min (Y. Zhang et al., 2014). An *n*-alkane mixture (C_{10}–C_{34}, 100 mg/l) was used as external standard for quantification and peak identification. The lipids were assigned by comparing their retention times and mass spectra with those of reference compounds. Concentrations of individual lipids were obtained by comparing their GC peak areas with those of the known reference compounds.

2.5. Lipid paleoclimate proxies

We employed a suite of *n*-alkane and *n*-alkanoic acid molecular ratios as proxies to help identify changes in the origins of the biomarkers and in their relative extents of preservation that could be sensitive to climate change. The two lipid classes have two proxies in common, and they each have several proxies that are specific to each class.

One of the shared proxies is the lipid CPI values that summarize the relative proportions of odd and even chain length *n*-alkanes (CPI-ALK) and even and odd *n*-FAs (CPI-FA) as follows (Zhou et al., 2010):

$$\text{CPI-ALK} = \sum C_{21-33} \quad (\text{odd}) \Big/ \sum C_{22-32} \quad (\text{even}) \tag{1}$$

$$\text{CPI-FA} = \sum C_{16-28} \quad (\text{even}) \Big/ \sum C_{17-29} \quad (\text{odd}) \tag{2}$$

where C_i is the concentration of the *n*-alkane or *n*-FA having i carbon atoms.

Lipid CPI values can record both the origin of the biomarker lipids and their degree of post depositional alteration in peat sequences (Zheng et al., 2007; Zhou et al., 2010). In general, lipids from terrestrial vascular plants have high CPI values, whereas lipids from bacteria and algae have low CPI values (Cranwell et al., 1987). However, lipid preservation in peat is commonly affected by microbial activity to some degree. *n*-FAs in sediments and peat have been postulated to be particularly sensitive indicators for reconstruction of paleoenvironmental conditions because carboxylic acids are more sensitive to degradation than other lipid biomarkers (Meyers and Ishiwatari, 1993; Zhou et al., 2005). Hence, the degree of preservation of *n*-FAs in sediments is closely related to factors affecting microbial degradation (Xie et al., 2004; Zhou et al., 2005, 2010; Zheng et al., 2007). Total concentrations of lipids and their CPI values can therefore indicate the extent of microbial degradation, which is postulated to reflect warmer climates more than cold ones (Zheng et al., 2007; Zhou et al., 2010).

Another shared proxy is ACL, the weighted mean chain length, which is also a useful proxy for reconstructing past change in the regional climate conditions under which different types of peat-forming plants developed (Andersson et al., 2011). The fundamental idea of ACL is that terrestrial vascular plants in warmer climate conditions often synthesize longer chain wax lipids than those in colder climate conditions as a strategy to help decrease loss of water by way of evapotranspiration (Gagosian and Peltzer, 1986). It is expressed as follows:

$$\text{ACL} = \sum (C_i \times [C_i]) \Big/ \sum [C_i] \tag{3}$$

where $[C_i]$ is the concentration of the *n*-alkane of carbon number C_i over the range 21–33 and of the *n*-acid of carbon number C_i over the range 16–28.

The P_{aq} is a paleoclimate proxy specific to *n*-alkanes that is calculated from *n*-alkane biomarker abundances (Ficken et al., 2000) and expressed as follows:

$$P_{aq} = (C_{23} + C_{25})/(C_{23} + C_{25} + C_{29} + C_{31}) \tag{4}$$

where C_i is the concentration of *n*-alkane of i number of carbons. P_{aq} has been effectively used to estimate the proportion of submerged or floating macrophytes that are more abundant in *n*-C_{23} and *n*-C_{25} relative to terrigenous vascular plants that are characterized by *n*-C_{29} and *n*-C_{31} (Cranwell, 1984; Ficken et al., 1998; Nott et al., 2000; Bass et al., 2000; Nichols et al., 2006; Bingham et al., 2010). Changes in P_{aq} values are therefore useful for reflecting water level history of peat-forming plants in peatlands (Zhou et al., 2010).

One proxy specific to *n*-FAs is the ratio of high/low molecular weight (H/L) *n*-FAs, based on the principle that aquatic algae or bacteria contain abundant short chain (C_{14}, C_{16} and C_{18}) *n*-FAs, whereas the lipids of terrigenous higher plants are dominated by long chain (C_{24}, C_{26} and C_{28}) homologues. The ratio can therefore represent the proportion of terrigenous vascular plants relative to aquatic algae and therefore might be used to estimate the paleohydrologic changes in a peat sequence (Cranwell, 1973). It is expressed as follows:

$$\text{H/L} = (C_{24} + C_{26} + C_{28})/(C_{14} + C_{16} + C_{18}) \tag{5}$$

where C_i is the concentration of *n*-alkane or *n*-FA of i number of carbons.

For the final proxy, we explored the concentration of the *n*-C_{15} FA as a biomarker to indicate microbial activity. Our basis for exploring its potential is the documentation that its carbon isotopic value is lower than that of the *n*-$C_{16:0}$ to *n*-$C_{28:0}$ in peat from the Ruoergai Marsh and in sediments from the Nansha Sea (Duan et al., 1997), hence suggesting a bacterial origin. Zheng et al. (2007) also inferred that the contribution of *n*-C_{15} FA in the Hongyuan peat sequence could indicate microbial contributions related to climate change. We therefore postulate that a greater concentration of *n*-C_{15} FA to the SJD peat might serve as a lipid proxy of intensified microbial activity and hence be indicative of warmer and more aerobic drier conditions.

3. Results

3.1. Chronology, PAR and TOC concentration in peat-mud sequence

The SJD peat-mud sequence represents a ca. 8 ky record of change in accumulation of peat-forming vegetation remains (Fig. 2). Before ca. 4 ka, the PAR was very slow and increased to a maximum from ca. 2 to 1.5 ka. Accumulation was again slow from 1.5 ka to the present (Fig. 2). TOC concentrations is between 2% and 10% in the sediments from black mud peat section (Fig. 2). Markedly higher TOC values occur in the peat section. They fluctuate widely between 15% and 35% in the basal peat deposited from 165 cm to 100 cm and then tend to be steady at ca. 40% from 100 cm to 15 cm. TOC concentration decreases to ca. 10% in the upper 15 cm.

3.2. n-Alkane concentration and distributions

The *n*-alkane distributions in the sequence range from C_{15} to C_{33} with a strong dominance of C_{27} and C_{29} (Fig. 3). In the upper peat unit starting at 20 cm, mid- and long chain length C_{21}, C_{23}, C_{25}, C_{27}, C_{29} and C_{31} *n*-alkanes are the major components, and these 6 homologues are in subequal proportions. In contrast, the distributions in the black muddy sediment layer at the bottom of the core are dominated by C_{25} and have abundant short chain *n*-alkanes with an even dominance.

Total *n*-alkane concentration ranges widely from 2 to 148 μg/g dry sediment over the sequence (Fig. 4). We use two different scales for the y-axis in this figure to compensate for the large change in sediment accumulation rate at ca. 2 ka and thus to better illustrate the variation in each proxy in the sequence. Before 1.5 ka, the concentration has lower values (< 10 μg/g), except for ca. 2.0 ka, when relatively high values (ca. 30 μg/g) exist. The values are relatively high at ca. 25 μg/g in the peat deposited since 1.5 ka, and the highest concentration (ca.150 μg/g) occurs at ca. 1.4 ka. When normalized to TOC, the total *n*-alkane concentration is generally < 0.1 mg/g TOC except in peat deposited at ca. 1.4 ka BP and in the black mud peat section, where it approaches 0.4 mg/g TOC (Fig. 4).

The *n*-alkane CPI values vary between 0.5 and 7.0, and most are > 2.0, corresponding to an obvious odd predominance in general (Figs. 3 and 4). ACL values range from 25.5 to 29.2, and the P_{aq} values from 0.2 to 0.7 over the whole sequence. Before ca. 6 ka, relatively low *n*-alkane CPI values but high ACL and P_{aq} values exist. After then, *n*-alkane CPI values increase and ACL decreases, but high P_{aq} values persist between 6 and 4 ka. From 4 to 1.5 ka, lower *n*-alkane CPI and higher ACL values appear and accompany relatively lower P_{aq} values. At ca. 2 ka, *n*-alkane P_{aq} values increase markedly and reach their maxima, CPI and ACL values sharply decrease and have obviously lower values at this time. During the period between 1.5 and 0.4 ka, relatively higher *n*-alkane CPI values but lower ACL values and higher P_{aq} values exist. Both

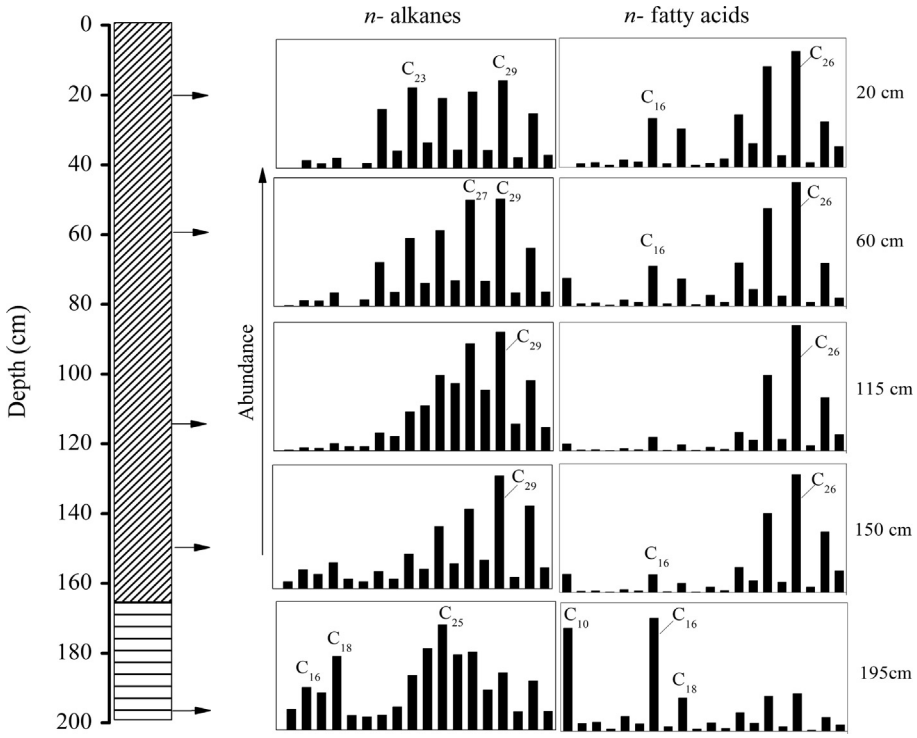

Fig. 3. Representative distributions of *n*-alkanes and *n*-FAs from peat samples in different units of the SJD peat sequence. Abundance of each component is relative to the major peak in each distribution.

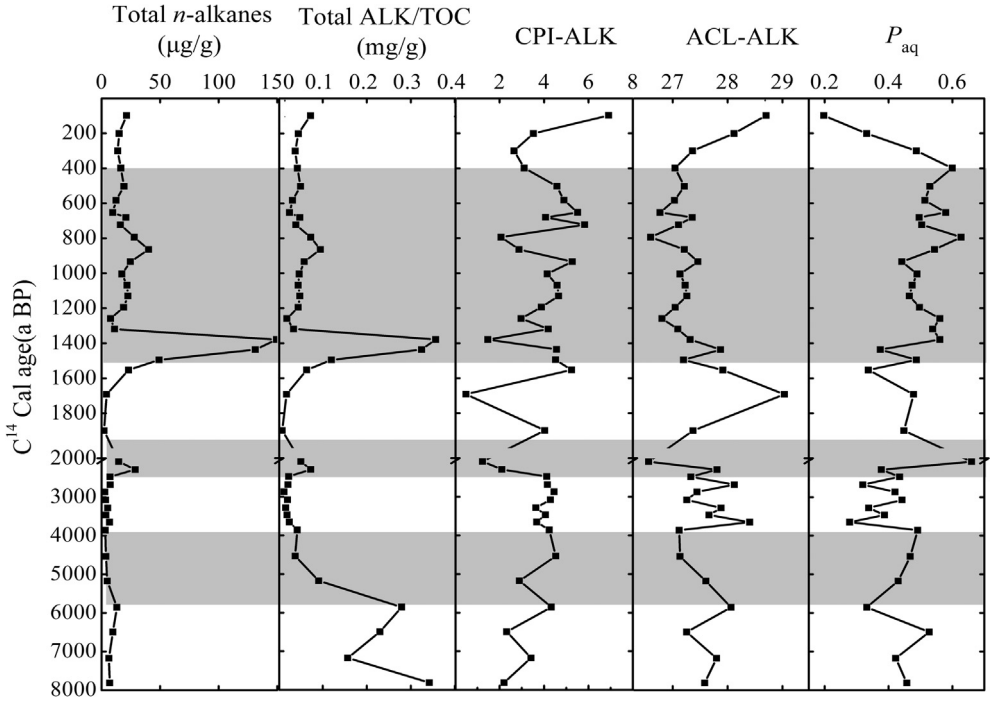

Fig. 4. Distribution of concentration of total *n*-alkanes (μg/g sediment), ratio of concentration of total *n*-alkanes to TOC (Total ALK/TOC, mg/g), CPI, ACL, P_{aq} values of *n*-alkanes (ALK) in SJD peat sequence. The unshaded and gray shaded areas represent warm/dry and cold/wet climate conditions in different periods during the Holocene, respectively.

n-alkane CPI and ACL subsequently increase, but P_{aq} values decrease sharply in the last 0.4 ky (Fig. 4).

3.3. n-FA concentration and distributions

The *n*-FA distributions range from C_{10} to C_{28}. The major FAs in the peat layers are dominated by C_{24}, C_{26} and C_{28}, but in the black muddy sediments they are dominated by *n*-C_{10} and *n*-C_{16} (Fig. 3). The concentration of total *n*-FAs varies widely between 2.5 μg/g and 494 μg/g dry sediment (Fig. 5). The concentrations are generally an order of magnitude larger than those of the *n*-alkanes (Fig. 4). We again use two different scales for the y-axis to compensate for the large change in sediment accumulation rate at ca. 2 ka and thus to better illustrate variation in *n*-FA content in the

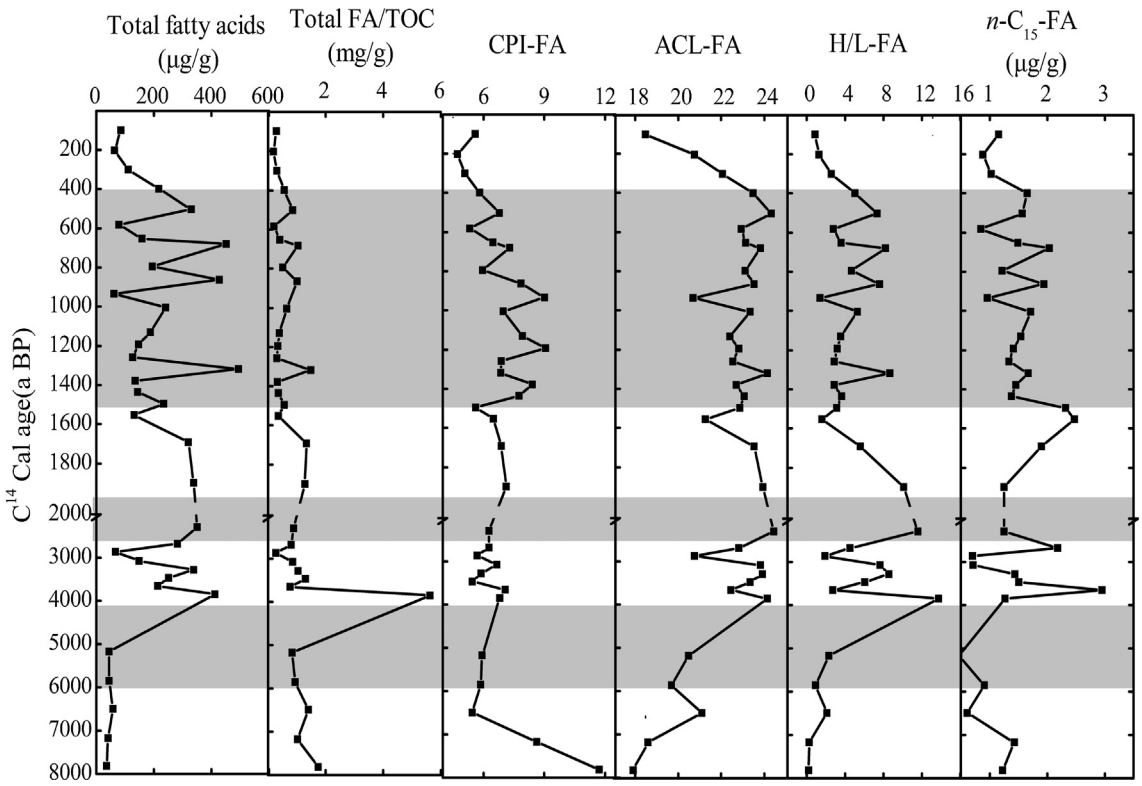

Fig. 5. Distribution of concentration of total *n*-FAs (μg/g sediment), ratio of concentration of total *n*-FAs to TOC (Total FA/TOC, mg/g), CPI, ACL, H/L values of *n*-FAs, concentration of C_{15} in SJD peat sequence. TOC data are from Z. Zhang et al. (2014); total concentration of *n*-FAs, CPI, ACL, H/L values of *n*-FAs and concentration of C_{15} data are from this study. The unshaded and gray shaded areas represent warm/dry and cold/wet climate conditions in different periods during the Holocene, respectively.

sequence. The concentration varies widely throughout the peat layers that first appear at ca. 4 ka, whereas the black muddy sediments have consistently low values. The TOC-normalized *n*-FA concentration ranges between 0.5 and 1.5 mg/g TOC in most of the peat layers, but maximizes at nearly 6 mg/g TOC at the onset of peat deposition. The normalized concentration in the black muds is 1–2 mg/g TOC, slightly higher than in the overlying peat (Fig. 5).

A strong even predominance contributes to higher *n*-FA CPI values that vary between 4.1 and 11.8 over the whole sequence (Figs. 3 and 5). The ACL values range from 17.9 to 25.3, and the H/L values fluctuate widely between 0.2 and 13.8 (Fig. 5). The CPI has its highest values and the ACL is at its lowest in the black mud sediments deposited before 4 ka. The *n*-FA H/L values exhibit changes similar to the ACL values, displaying their lowest values in this phase. Pronounced increases in *n*-FA total concentration and the ACL and H/L values occur in the peat sequence, but the CPI drops from higher values in the black mud peat to lower ones in the peat. At the same time, the concentration of *n*-C_{15} FA decreases to its minimum in the whole sequence between 6.0 to 4.0 ka. *n*-FA CPI values vary between 5 and 7 from 4.0 to 1.5 ka, but H/L reaches the highest values in this period. Meanwhile, *n*-C_{15} FA values increase to a maximum. The time between 1.5 and 0.4 ka is characterized by relatively high total *n*-FA concentration and CPI and ACL values, but low *n*-C_{15} FA and H/L values. All the *n*-FA proxies decrease sharply during the last 0.4 ky (Fig. 5).

4. Discussion

4.1. Lipid biomarker origin

TOC concentration can serve as an indicator for reflecting the kind and amount of different types of local vegetation. In general, terrigenous vascular plants could produce more TOC than aquatic organisms (Chai, 1990). Therefore, we hypothesize that the stable lower TOC and total lipid sediment concentrations and higher ratio values for total *n*-alkanes and total *n*-FAs relative to TOC in the black peaty mud section from 195 cm to 165 cm of the core (Figs. 2, 4 and 5) imply an origin from algae and microbes that produced less TOC rather than from TOC-rich terrigenous vascular plants (Chai, 1990). Meanwhile, the distributions of the *n*-alkanes and *n*-fatty FAs also suggest the origin of this organic matter (Fig. 3); the *n*-alkane distributions have a low contribution from the long chain *n*-alkanes that are diagnostic of land plant wax (e.g. Eglinton and Hamilton, 1967) and are dominated instead by short and mid- chain *n*-alkanes C_{16}, C_{18} and C_{25} that are typical of aquatic organisms (e.g. Ficken et al., 2000; Liu and Liu, 2016); the FA distributions in this part of the sequence similarly have a low contribution from land plant components and instead have a greater abundance of short chain components that are common in aquatic algae or bacteria (Cranwell et al., 1987; Zhou et al., 2005). In addition, the significant proportions of C_{16} and C_{18} *n*-alkanes are generally unusual in the biosphere and geosphere (e.g. Lu and Meyers, 2009). These compounds have been isolated from the diatomaceous oozes of a freshwater lake by Grimalt and Albaiges (1987), who postulated a microbial origin for these unusual *n*-alkanes. They have also been isolated from oil-contaminated sediments from a Nigerian river (Ekpo et al., 2005) and from Lake Erie (Lu and Meyers, 2009), where their origin from microorganisms inhabiting these oil-polluted sediments was postulated. Because the SJD peatland, a relatively closed area in the Sanjiang Plain, is little influenced by human activity, and no local natural petroliferous sources are known, the deposition of the SJD peat sequence is very unlikely to have been contaminated by petroleum. Therefore, we conclude that pristine populations of microbes are the probable source of the even chain *n*-alkanes in these black muddy sediments

(Fig. 3). Taking these lines of information together, the *n*-alkane and *n*-FA sedimentary distributions in the bottom of the SJD sequence therefore both suggest an important origin from algae and microbes. In addition, Wang et al. (2015) noted that remains of the water plant *Equisetum fluviatile* constitute the dominant macrofossil found in this portion of the core. These features collectively indicate an aquatic origin for the *n*-alkanes and *n*-FAs in the basal sediment in the SJD sequence and reflect their deposition in a shallow lake setting.

In addition to differing in TOC-normalized concentration, the distributions of the *n*-alkanes and *n*-FAs in the peat-rich upper 165 cm of the core differ from those in the basal sediment (Figs. 3–5). These features imply a major input to the peat from terrigenous vascular plant wax characterized by TOC-rich organic matter and long chain lipids (Eglinton and Hamilton, 1967). In support of this interpretation, pollen assemblages in these sections are characterized by the highest proportions of herbaceous taxa (Zhang et al., 2015), and the macrofossil content of this part of the sequence is dominated by the sedge *Carex lasiocarpa* (Wang et al., 2015). In the upper peat unit, the dominance of mid- and long length carbon *n*-alkanes implies an origin mainly from a combination of *Sphagnum* spp. or submerged and floating vascular plants, plus terrigenous vascular plants (e.g. Nott et al., 2000; Bass et al., 2000; Nichols et al., 2006; Bingham et al., 2010). Pollen and macrofossil records from this portion of the sequence indicate that *Carex* spp. are the major contributors to the peat (Wang et al., 2015), yet large amounts of spores also appear in this part, as noted for the pollen data (Zhang et al., 2015). Therefore, we conclude that *Carex* spp. and *Sphagnum* spp are the major contributors of mid- and long chain lipids in the uppermost portion of the peat sequence. However, the small but significant contribution of the *n*-C_{16} FA to the upper brown peat portion (Fig. 3) may indicate enhanced microbial activity in this portion of the sequence (Zhou et al., 2005).

4.2. Paleoclimatic history of Sanjiang Plain based on lipid biomarker proxies

Z. Zhang et al. (2016) document a 6× increase in OC mass accumulation rate on the plain starting ca. 4.4 ka that they postulate reflects a weakening of summer monsoon rain and a consequent lake-to-peatland transition. The virtual absence of peat accumulation in the SJD core before ca. 4 ka is consistent with a much smaller input of plant biomass to this former lake basin than after that time (Fig. 2). The pattern mimics the record of carbon accumulation at core site SH that is at the same general area as the SJD and close to the SJD core site and evidently shares a similar hydrologic history (Z. Zhang et al., 2016). Both lower TOC values and lower total concentration of *n*-alkanes and *n*-FAs (Figs. 4 and 5) record low production of organic matter in this phase. Moreover, the lipid distributions in the bottom of the core exhibit a dominance of shorter chain *n*-alkanes and *n*-FAs (Fig. 3) that suggests a major input from bacteria and algae. High *n*-alkane P_{aq} (0.4–0.5) values provide more evidence of a high water level and a predominantly aquatic plant input of organic matter in this period (Fig. 4). Moreover, markedly elevated *n*-FA CPI values record good preservation of the *n*-acids in the sediment and imply weaker microbial degradation under permanently subaqueous conditions (Fig. 5) that correspond to a lower humification degree recorded by Wang et al. (2015). At the same time, algae were major contributors and some microbes were active, as indicated by the lowest *n*-FA ACL and H/L values and prominently higher *n*-C_{15} FA values (Fig. 5). In addition, the dominance of the aquatic macrophyte *Equisetum fluviatile* in this period (Wang et al., 2015) suggests that this portion of the SJD peatland accumulated in a shallow lake or pond. This interpretation is also consistent with the conclusions of Z. Zhang et al. (2016) for nearby core site SH.

During the mid-Holocene (6–4 ka), the regional climate was characterized by cold and relatively wet conditions as deduced from increased *n*-alkane CPI and P_{aq} values and decreased ACL values in the sequence (Fig. 4). Lowest *n*-C_{15} FA values suggest weaker microbial activity in response to cold and wet conditions (Fig. 5). This interpretation is supported by lower humification values in the Shenjiadian peat (Wang et al., 2015). Although wet conditions still existed from 6 to 4 ka, the water level was dropping, as suggested by pronounced increases in total concentration of the lipids and *n*-FA ACL and H/L values that indicate terrigenous higher plants began to become important contributors of lipids to the sequence (Figs. 4 and 5). Pollen and plant macrofossil records from the peat reflect important amounts of *Carex* spp. during this period (Zhang et al., 2015; Wang et al., 2015). Taking these lines of evidence together, aquatic macrophytes still existed, but contributions from terrigenous higher plants increased in this period, indicating that the lake had shallowed and a lake–to-wetland transition began in the basin as early as 6 ka.

The SJD peat sequence accumulated rapidly during the mid-late Holocene after 4 ka, as recorded by the TOC values and PAR values that both increased markedly (Fig. 2). Vegetation in the region was dominated by *Carex* spp. instead of aquatic plants, as indicated by plant macrofossil data (Wang et al., 2015). The climate in the region entered into a long warm and dry period associated with a large contribution of organic matter from terrigenous higher plants with long chain lipids during this period as recorded by the highest ACL values (Figs. 4 and 5). Lowering of the peatland water level occurred in this period, as evident from the lower *n*-alkane P_{aq} and much higher *n*-FA H/L values, indicating that few aquatic and hygrophilous plants were present. Poor preservation of lipids in this period is suggested by relatively lower total concentrations of both *n*-alkanes and *n*-FAs and lower lipid CPI values, particularly the lowest *n*-alkane CPI values that represent intensified microbial degradation under warm and dry conditions (Figs. 4 and 5). Moreover, higher *n*-C_{15} FA values also indicate stronger microbial activity (Fig. 5). This interpretation is supported by increased humification values in the peat (Wang et al., 2015). However, it is worth noting that an obvious colder and wetter transitional stage appears to have occurred at ca. 2 ka as recorded by lower lipid CPI and ACL values and the highest *n*-alkane P_{aq} values that collectively indicate that aquatic and hygrophilous plants or mosses reappeared, suggesting that the climate again entered cold and wet conditions (Fig. 4). Well preserved lipids suggested by higher total *n*-alkane and *n*-FA concentrations and lower *n*-C_{15} FA values at ca. 2 ka also reflect weak microbial activity related to cold and poorly aerated wetter conditions (Figs. 4 and 5).

In the SJD peat sequence, higher and more stable TOC concentration accumulated during the late Holocene (1.5–0.4 ka) (Fig. 2), recording relatively well preserved organic matter. Lipid biomarker distributions show that the highest total concentration and higher CPI of both *n*-alkanes and *n*-FAs occur in this period (Figs. 4 and 5), indicating good preservation of lipids in the peat, presumably associated with weakened microbial degradation under cold and wet climate conditions. This assumption is supported by lower *n*-C_{15} FA values (Fig. 5). However, Wang et al. (2015) emphasized that the water level of the peatland decreased, as recorded by plant macrofossil proxies and higher peat humification values that would be related to intensified microbial degradation in this stage. We postulate that peat organic matter accumulation was greater than microbial decomposition rate during this period of moderate climate. Lower ACL values (< 27) with higher P_{aq} values indicate the presence of submerged and floating aquatic macrophytes or mosses with *n*-alkane distributions dominated by mid-chain homologs, but fewer aquatic algae existed, as suggested by higher *n*-FA ACL and H/L values (Figs. 4 and 5). Taking these data together, we hypothesize that mosses with high organic

matter content that were more recalcitrant to microbial degradation probably were the major contributors to the peat because of cold and wet conditions on the Sanjiang Plain during the late Holocene.

In the most recent 0.4 ky, palynology shows a higher proportion of spores, indicative of mosses, and a decrease in herb and tree pollen (Zhang et al., 2015). However, the plant macrofossil record shows significant increases in *Carex* spp. (Wang et al., 2015). Our lipid results show a marked increase in *n*-alkane CPI and ACL values but a decrease in P_{aq} values, both of which could be related to a major development of terrigenous higher plants. Lower total *n*-alkane and *n*-FA concentrations might result from poor preservation of organic matter associated with strong microbial activity under warmer and drier climate conditions (Figs. 4 and 5). This climate character also corresponds to a decrease in TOC values and higher humification values that indicate poor preservation of organic matter in peat because of stronger microbial activity (Z. Zhang et al., 2014; Wang et al., 2015), leading to lower PAR values (Fig. 2). Notably, an obvious decrease occurred in *n*-FA CPI, ACL and H/L values at this time (Fig. 5), indicating poor preservation of the original plant biomarker acids. The *n*-FAs in this period might be secondary acids that formed from primary acids after decomposition as a consequence of intensified microbial activity, or some combination of these alteration processes (Zhou et al., 2005, 2010).

4.3. Regional climate comparisons and possible causes for Holocene climate change on the SJP

Several paleoclimate reconstructions exist for parts of northeastern China close to the SJP. Zhou et al. (2010) used the biomarker composition of the peat sequence in Hani peatland to assess the paleoclimatic evolution of the region. Peat cellulose $\delta^{13}C$ values in the Jinchuan peatland have been used to reconstruct the humidity history in the region based on the response of the relative proportions of C_3 and C_4 plants to variation in relative humidity or effective precipitation (Hong et al., 2001). In addition, pollen data from the Hulun Lake and Sihailongwan Maar Lake sediment records were used to reconstruct the paleoclimate of northeast China (Wen et al., 2010; Stebich et al., 2015).

During the early and middle Holocene (8–6 ka), the TOC and lipid distributions of the SJD peat sequence indicate that greater effective moisture promoted abundant aquatic plant and algal development when the study site was an open shallow lake environment. Higher ACL *n*-alkane values from the SJD and Hani peat cores indicate warmer conditions in northeast China, coinciding with the highest SST in the Sea of Japan at this time related to strong insolation at 65°N (Fig. 6). Zhou et al. (2010) postulated that local SST changes in the Sea of Japan could not only reflect the temperature in the adjacent region of northeast China but also might have influenced effective precipitation over these areas. The wetter conditions that occurred in northeast China during the early-mid Holocene could therefore be related to a higher local SST of the Sea of Japan that enhanced evaporation and consequently increased precipitation in the region. An important increase in precipitation evidently occurred in the Hulun Lake and Sihailongwan Maar Lake regions of northeast China during the early and middle Holocene (Wen et al., 2010; Stebich et al., 2015). The higher *n*-alkane P_{aq} values in the SJD peat imply wetter climate conditions during this warmer period, which is in general associated with the Holocene Thermal Optimum and wetter climate elsewhere in East Asia (Herzschuh, 2006; Jiang et al., 2006; Zhou et al., 2010). The timing of the highest Holocene SST in the Sea of Japan corresponds with the lowest stalagmite $\delta^{18}O$ values for Dongge Cave that are indicative of the strongest East Asia summer monsoon during the Holocene (Fig. 6). Taking these data together, the warmer and wetter climate conditions before ca. 6 ka on the SJP could be related to the higher local SST of the Sea of Japan and the occurrence of a stronger East Asia summer monsoon during this stage, corresponding with the monsoon maximum and Holocene climate optimum during the early-mid Holocene (Zhou et al., 2010; Zhao et al., 2011).

During the mid-Holocene (6–4 ka), lower ACL values in both the SJD peat and the Hani peat (Fig. 6) indicate a cold climate in northeast China, corresponding to the lowest SST values of the Sea of Japan and decreased solar insolation (Fig. 6). At the same time, wet climate conditions in northeast China are indicated by relative high *n*-alkane P_{aq} values from the SJD and the Hani peat sequences and more negative peat cellulose $\delta^{13}C$ values in the Jinchuan peat sequence (Fig. 6). A relatively strong East Asia summer monsoon during this period may have contributed to much regional precipitation, yet rainfall became weaker than before as recorded by way of Dongge Cave stalagmite $\delta^{18}O$ values greater than the values in the early-mid Holocene before 6.0 ka (Fig. 6). We therefore postulate that, although wet conditions still existed in this period, the precipitation in our study region was much less than before, as evidenced by the shoaling of the former shallow lake because of the lower Sea of Japan SST that suppressed oceanic evaporation and led to a gradual decrease in the Asian summer monsoon rains.

During the mid-late Holocene (4.0–1.5 ka), higher ACL *n*-alkane values in the SJD and Hani peat imply a greater development of terrigenous higher plants under warmer climate conditions in close association with the relatively high SST of the Sea of Japan (Fig. 6). In the SJD peat sequence, higher TOC concentration since ca. 4.0 ka indicates a transformation from a lake environment to a peatland, which in turn implies a change to less wet conditions in the Sanjiang region. Lower *n*-alkane P_{aq} values in both the SJD and Hani peat sequences and higher peat cellulose $\delta^{13}C$ values in the Jinchuan peat also indicate a shift to a climate that was somewhat drier than before, coinciding with a weakening in the East Asia summer monsoon that is reflected in a gradual increase in stalagmite $\delta^{18}O$ values from the Dongge Cave (Fig. 6). Drier climate in northeast China in this period is also indicated by pollen records from Hulun Lake (Wen et al., 2010) and Sihailongwan Maar Lake (Stebich et al., 2015) because of a weakening of the East Asia summer monsoon. However, it is worth mentioning that a shift to cooler and wetter climate conditions occurred at ca. 2 ka, as evidenced by good preservation of organic matter and prominent *n*-alkane proxy values in the SJD and Hani peat sequences (Fig. 6). This transitory cold stage in northeastern China also corresponds to lower SST in the Sea of Japan (Fig. 6).

In the late Holocene (1.5–0.4 ka), good preservation of organic matter in the SJD peat is likely a result of weaker microbial degradation because of the cooler conditions in northeast China, as indicated by lower *n*-alkane ACL values in both the SJD and the Hani peat sequences. This millennial-scale cold period is consistent with lower SST in the Sea of Japan and is synchronized with weaker summer solar insolation (Fig. 6). Moreover, higher *n*-alkane P_{aq} values in the SJD peat indicate the climate in the Sanjiang region entered a wet period. This cold and humid condition in northeast China during the late Holocene was also reported from the Hani peat lipid composition and Jinchuan peat cellulose $\delta^{13}C$ values, which are associated with a gradually strengthening summer monsoon, as also evidenced from decreased stalagmite $\delta^{18}O$ values in the Dongge Cave in this period (Fig. 6).

Our lipid biomarker records suggest a warmer and drier climate in the Sanjiang region since 0.4 ka BP. Lipid results from the SJD peat share approximately the same ACL and P_{aq} values as the Hani peat (Fig. 6), both signifying a warmer and drier climate period in northeast China, together with higher peat cellulose $\delta^{13}C$ values in Jinchuan peat (Fig. 6). Also, pollen records in Hulun Lake provide support for a warmer regional climate (Wen et al., 2010). However, *n*-alkane proxies in the Great Hinggan Mountain ombrotrophic

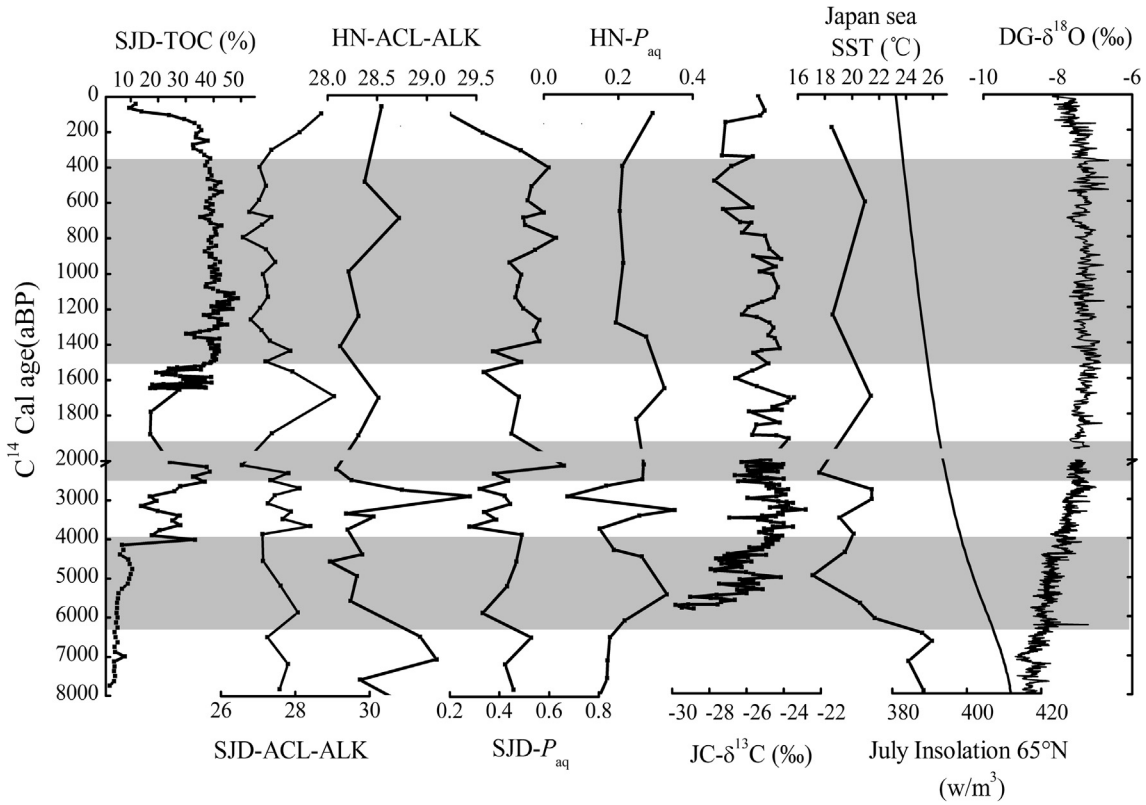

Fig. 6. Comparison of SJD *n*-alkane biomarker ACL and P_{aq} proxies with TOC concentration, *n*-alkane ACL and P_{aq} proxies from Hani (HN) peat sequence, peat cellulose $\delta^{13}C$ values in the Jinchuan (JC) peat sequence, Sea of Japan sea surface temperature (SST), July insolation at 65°N, and stalagmite $\delta^{18}O$ values of the Dongge (DG) Cave. The SJD-TOC data are from Z. Zhang et al. (2014). The SJD-ACL-ALK and SJD-P_{aq} data are from this study. The HN-ACL-ALK and HN-P_{aq} data are from Zhou et al. (2010). The JC-$\delta^{13}C$ data are from Hong et al. (2001). The SST data for the Sea of Japan are from Ishiwatari et al. (2001). July insolation data at 65°N are from Berger and Loutre (1991). The DG $\delta^{18}O$ data are from Wang et al. (2005).

peat bog suggest that the climate entered cold and wet conditions in recent years in parts of northeast China (Y. Zhang et al., 2014). Moreover, the warm and dry climate characteristics of the Sanjiang Plain in recent years are not consistent with the lower SST of the Sea of Japan and the increased summer monsoon rains (Fig. 6). Hong et al. (2001) pointed out that the regional warm and dry climate in northeast China has also recently been affected by an expanded population with stronger industrial and agricultural activity. Wen et al. (2010) and Z. Zhang et al. (2016) also suggested that human activity might have had a significant influence on the environment in recent years. In the Sanjiang Plain, field burning associated with the Han farming culture increased rapidly during the last millennium (Cong et al., 2016). In addition, several notable wars occurred on the northwestern Sanjiang Plain that caused eastward population relocation in the past few centuries (Sun and Liu, 1994; Li and Yuan, 1996). Therefore, we suggest that anthropogenic activity has now become a major factor in causing the recent change to a warm and dry climate evident in sedimentary records of the Sanjiang Plain.

5. Conclusions

Lipid biomarker analysis of the SJD peat sequence from the Sanjiang Plain in northeast China provides evidence that allows a more detailed reconstruction of the history of regional climate changes since 8 ka. A combination of *n*-alkane and *n*-FA distributions and ratios and other published climate proxies for the SJD peat was employed to assess the change in lipid distributions in the peat sequence in response to paleoclimate changes in the region. Before ca. 6 ka, the distributions in the peat suggest considerable aquatic plant input from the relatively high concentration of short chain homologs of lipids, suggesting warmer and wetter climate conditions that correspond to the monsoon maximum and Holocene climate optimum during the early-mid Holocene. This early stage in the depositional history evidently was lacustrine. The climate entered a cold and wet period starting 6 ka during which aquatic macrophytes also existed, but an increasingly greater contribution from terrigenous higher plants began to develop in the region as the lake became shallower. Because of a transformation from a lake environment to a peatland, a large amount of terrigenous higher plants with long chain homologues of lipids developed, suggesting the regional climate entered a long term warm and dry period between 4 and 1.5 ka. However, an interlude of transitory colder and wetter condition occurred at ca. 2 ka. In the period from 1.5 to 0.4 ka, a millennial-scale cold and wet climate conditions occurred, as suggested by good preservation of lipids in peat. In the most recent 0.4 ky, a significant input from terrigenous plants greatly contributed to long chain lipid preservation in the peat, displaying a close link with the warmer and drier climate conditions that would have enhanced microbial degradation and thereby diminished organic matter preservation in the peat.

A regional climate comparison indicates that the paleoclimate information inferred from lipid biomarkers in the SJD peat sequence is consistent with the biomarker-based Holocene climate reconstruction from the Hani peat sequence and isotope-inferred climate record from the Jinchuan peat sequence and published pollen records from lakes of northeast China. The climate changes during the Holocene in the Sanjiang Plain are in close correspondence to the variation in Sea of Japan SST related to summer solar insolation and the East Asia summer monsoon. However, the evidence for a shift to warmer and drier conditions in the region in the last

four centuries seems to be mainly associated with anthropogenic activity.

Acknowledgments

We thank the two anonymous reviewers for thoughtful suggestions. We gratefully acknowledge the Analysis and Test Center of Northeast Institute of Geography and Agroecology, Chinese Academy of Sciences, for sample analysis. The study relied on funds from the National Key Research and Development Project (No. 2016YFA0602301) and the National Natural Science Foundation of China (no. 41571191; 41271209), the National Basic Research Program of China (no. 2012CB956103).

Associated Editor—**B. van Dongen**

References

Andersson, R.A., Kuhry, P., Meyers, P., Zebühr, Y., Crill, P., Mörth, M., 2011. Impacts of paleohydrological changes on *n*-alkane biomarker compositions of a Holocene peat sequence in the eastern European Russian Arctic. Organic Geochemistry 42, 1065–1075.

Bass, M., Pancost, R., van Geel, B., Sinninghe-Damsté, J., 2000. A comparative study of lipids in *Sphagnum* species. Organic Geochemistry 31, 535–541.

Berger, A., Loutre, M.F., 1991. Insolation values for the climate of the last 10 million years. Quaternary Science Reviews 10, 297–317.

Bingham, E.M., McClymont, E.L., Väliranta, M., Mauquoy, D., Roberts, Z., Chamber, F. M., Pancost, R.D., Evershed, R.P., 2010. Conservative composition of *n*-alkane biomarkers in *Sphagnum* species: implications for palaeoclimate reconstruction in ombrotrophic peat bogs. Organic Geochemistry 41, 214–220.

Blackford, J., 2000. Palaeoclimatic records from peat bogs. Trends in Ecology & Evolution 15, 193–198.

Chai, X., 1990. Peat-geology. Geological Publishing House, Beijing, pp. 136–309 (in Chinese).

Cong, J.X., Gao, C.Y., Zhang, Y., Zhang, S.Q., He, J.B., Wang, G.P., 2016. Dating the period when intensive anthropogenic activity began to influence the Sanjiang Plain, Northeast China. Scientific Reports 6, 1–10.

Cranwell, P.A., 1973. Chain-length distribution of *n*-alkanes from lake sediments in relation to post-glacial environmental change. Freshwater Biology 3, 259–265.

Cranwell, P.A., 1984. Lipid geochemistry of sediments from Upton Broad, a small productive lake. Organic Geochemistry 7, 25–37.

Cranwell, P.A., Eglinton, G., Robinson, N., 1987. Lipids of aquatic organisms as potential contributors to lacustrine sediments. Organic Geochemistry 11, 513–527.

Duan, Y., Wen, Q.B., Luo, B.J., 1997. Isotopic composition and probable origin of individual fatty acids in modern sediments from Ruoergai Marsh and Nansha Sea, China. Organic Geochemistry 27, 583–589.

Eglinton, G., Hamilton, R.J., 1967. Leaf epicuticular waxes. Science 156, 1322–1334.

Ekpo, B.O., Oyo-Ita, O.E., Wehner, H., 2005. Even *n*-alkane predominances in surface sediments from the Calabar River, SE Niger Delta. Naturwissenschaften 92, 341–346.

Ficken, K.J., Barber, K.E., Eglinton, G., 1998. Lipid biomarker, $\delta^{13}C$ and plant macrofossil stratigraphy of a Scottish montane peat bog over the last two millennia. Organic Geochemistry 28, 217–237.

Ficken, K.J., Li, B., Swain, D.L., Eglinton, G., 2000. An *n*-alkane proxy for the sedimentary input of submerged/floating freshwater aquatic macrophytes. Organic Geochemistry 31, 745–749.

Gagosian, R.B., Peltzer, E.T., 1986. The importance of atmospheric input of terrestrial organic material to deep sea sediments. Organic Geochemistry 10, 661–669.

Grimalt, J., Albaiges, J., 1987. Sources and occurrence of C_{12}–C_{22} normal-alkane distributions with even carbon-number preference in sedimentary environments. Geochimica et Cosmochimica Acta 51, 1379–1384.

Herzschuh, U., 2006. Palaeo-moisture evolution in monsoonal Central Asia during the last 50,000 years. Quaternary Science Reviews 25, 163–178.

Hong, B., Liu, C.Q., Lin, Q.H., Yasuyuki, S., Leng, X.T., Wang, Y., Zhu, Y.X., Hong, Y.T., 2009. Temperature evolution from the $\delta^{18}O$ record of Hani peat, Northeast China, in the last 14000 years. Science in China Series D: Earth Sciences 52, 952–964.

Hong, Y.T., Wang, Z.G., Jiang, H.B., Lin, Q.H., Hong, B., Zhu, Y.X., Wang, Y., Xu, L.S., Leng, X.T., Li, H.D., 2001. A 6000-year record of changes in drought and precipitation in northeastern China based on a $\delta^{13}C$ time series from peat cellulose. Earth and Planetary Science Letters 185, 111–119.

Hong, Y.T., Hong, B., Lin, Q.H., Shibata, Y., Hirota, M., Uchida, M., Zhu, Y.X., Leng, X.T., Wang, Y., Wang, H., Yi, L., 2005. Inverse phase oscillations between the East Asian and Indian Ocean summer monsoons during the last 12000 years and paleo-El Niño. Earth and Planetary Science Letters 231, 337–346.

Ishiwatari, R., Houtatsu, M., Okada, H., 2001. Alkenone-sea surface temperature in the Japan Sea over the past 36 kyr: warm temperatures at the last glacial maximum. Organic Geochemistry 32, 57–67.

Jiang, W., Gua, Z., Sun, X., Wu, H., Chu, G., Yuan, B., Hatté, C., Guiot, J., 2006. Reconstruction of climate and vegetation changes of Lake Bayanchagan (Inner Mongolia): Holocene variability of the East Asian Monsoon. Quaternary Research 65, 411–420.

Li, S., Yuan, Z., 1996. Historical Population in Heilongjiang Province. Heilongjiang Publishing Group, Heilongjiang, China (in Chinese).

Lin, Q.H., Leng, X.T., Hong, B., 2004. The peat record of 1 ka of climate change in Daxing Anling. Bulletin of Mineralogy, Petrology and Geochemistry 23, 15–18 (in Chinese).

Liu, X.T., 1995. Wetland and Its Rational Utilization and Conservation in the Sanjiang Plain. Jilin Science Technology Press, Changchun, pp. 108–117 (in Chinese).

Liu, H., Liu, W., 2016. *N*-Alkane distributions and concentrations in algae, submerged plants and terrestrial plants from the Qinghai-Tibetan Plateau. Organic Geochemistry 99, 10–22.

Lu, Y., Meyers, P.A., 2009. Sediment biomarkers as recorders of the contamination and cultural eutrophication of Lake Erie, 1909–2003. Organic Geochemistry 40, 912–921.

Meyers, P.A., Ishiwatari, R., 1993. Lacustrine organic geochemistry: an overview of indicators of organic matter sources and diagenesis in lake sediments. Organic Geochemistry 20, 867–900.

Nichols, J.E., Booth, R.K., Jackson, S.T., Pendall, E.G., Huang, Y.S., 2006. Paleohydrologic reconstruction based on *n*-alkane distributions in ombrotrophic peat. Organic Geochemistry 37, 1505–1513.

Nott, C.J., Xie, S., Avsejs, L.A., Maddy, D., Chambers, F.M., Evershed, R.P., 2000. *n*-Alkane distributions in ombrotrophic mires as indicators of vegetation change related to climatic variations. Organic Geochemistry 31, 231–235.

Seki, O., Meyers, P.A., Kawamura, K., Zheng, Y., Zhou, W., 2009. Hydrogen isotopic ratios of plant-wax *n*-alkanes deposited in a peat bog in northeastern China during the last 16 ky. Organic Geochemistry 40, 671–677.

Stebich, M., Rehfeld, K., Schlütz, F., Tarasov, P.E., Liu, J.Q., Mingram, J., 2015. Holocene vegetation and climate dynamics of NE China based on the pollen record from Sihailongwan Maar Lake. Quaternary Science Reviews 124, 275–289.

Sun, C., Liu, J., 1994. Historical military in Heilongjiang Province. Heilongjiang Publishing Group, Heilongjiang, China (in Chinese).

Wang, Y.J., Cheng, H., Edward, R.L., He, Y.Q., Kong, X.G., An, A.S., Wu, J.Y., 2005. The Holocene Asian monsoon: link to solar changes and North Atlantic climate. Science 308, 854–857.

Wang, C.L., Zhao, H.Y., Wang, G.P., 2015. Vegetation development and water level changes in Shenjiadian Peatland in Sanjiang Plain, Northeast China. Chinese Geograph Science 25, 451–461.

Wen, R., Xiao, J., Chang, Z., Zhai, D., Xu, Q., Li, Y., 2010. Holocene climate changes in the mid-high-latitude-monsoon margin reflected by the pollen record from Hulun Lake, northeastern Inner Mongolia. Quaternary Research 73, 293–303.

Xie, S., Nott, C.J., Avsejs, L.A., Maddy, D., Chambers, F.M., Evershed, R.P., 2004. Molecular and isotopic stratigraphy in an ombrotrophic mire for paleoclimate reconstruction. Geochimica et Cosmochimica Acta 68, 2849–2862.

Yamamoto, S., Kawamura, K., Seki, O., Meyers, P.A., Zheng, Y.H., Zhou, W.J., 2010. Paleoenvironmental significance of compound-specific $\delta^{13}C$ variations in *n*-alkanes in the Hongyuan peat sequence from southwest China over the last 13 ka. Organic Geochemistry 41, 491–497.

Zhang, Y., Liu, X.T., Lin, Q.X., Gao, C.Y., Wang, J., Wang, G.P., 2014. Vegetation and climate change over the past 800 years in the monsoon margin of northeastern China reconstructed from *n*-alkanes from the Great Hinggan Mountain ombrotrophic peat bog. Organic Geochemistry 8, 128–135.

Zhang, Y., Meyers, P.A., Liu, X., Wang, G., Ma, X., Li, X., Yuan, Y., Wen, B., 2016. Holocene climate changes in the central Asia mountain region inferred from a peat sequence from the Altai Mountains, Xinjiang, northwestern China. Quaternary Science Reviews 152, 19–30.

Zhang, Z., Zhao, M., Eglinton, G., Lu, H.Y., Huang, C.Y., 2006. Leaf wax lipids as paleovegetational and paleoenmental proxies for the Chinese Loess Plateau over the last 170 kyr. Quaternary Science Reviews 25, 575–594.

Zhang, Z., Xing, W., Lu, X.G., Wang, G.P., 2014. The grain-size depositional process in wetlands of the Sanjiang Plain and its links with the East Asian monsoon variations during the Holocene. Quaternary International 349, 245–251.

Zhang, Z., Wang, G., Liu, X., Jia, H., 2016. Holocene controls on wetland carbon accumulation in the Sanjiang Plain, China. Journal of Paleolimnology 56, 267–274.

Zhang, Z., Zhong, J.J., Lu, X.G., Tong, S.Z., Wang, G.P., 2015. Climate, vegetation, and human influences on late Holocene fire regimes in the Sanjiang plain, northeastern China. Palaeogeography, Palaeoclimatology, Palaeoecology 438, 1–8.

Zhao, Y., Yu, Z.C., Zhao, W.W., 2011. Holocene vegetation and climate histories in the eastern Tibetan Plateau: controls by insolation-driven temperature or monsoon-derived precipitation changes? Quaternary Science Reviews 30, 1173–1184.

Zheng, Y.H., Zhou, W.J., Meyers, P.A., Xie, S.C., 2007. Lipid biomarkers in the Zoigê-Hongyuan peat deposit: indicators of Holocene climate changes in West China. Organic Geochemistry 38, 1927–1940.

Zhou, W.J., Xie, S.C., Meyers, P.A., Zheng, Y.H., 2005. Reconstruction of late-glacial and Holocene climate evolution in southern China from geolipids and pollen in the Dingnan peat sequence. Organic Geochemistry 36, 1272–1284.

Zhou, W.J., Zheng, Y.H., Meyers, P.A., Jull, A.J., Xie, S.C., 2010. Postglacial climate-change record in biomarker lipid compositions of the Hani peat sequence, Northeastern China. Earth and Planetary Science Letters 294, 37–46.